

Reference

NBS
Publi-
cations

NAT'L INST OF STAND & TECH



A11101 726706

A11106 978798

NBSIR 78-1488

**Measurement Techniques for Solar
Cells,
Quarterly Report:
September 15 to December 31, 1977**

D. E. Sawyer, H. K. Kessler,
and H. A. Schafft

Electron Devices Division
Center for Electronics and Electrical Engineering
National Bureau of Standards
Washington, D.C. 20234

July 1978

-Final

Prepared for

Department of Energy
Washington, D.C. 20545

QC

100

.U56

78-1100



APR 17 1979

10-110-1301
09/15/77
70.9488

NBSIR 78-1488

**MEASUREMENT TECHNIQUES FOR SOLAR
CELLS,
QUARTERLY REPORT:
SEPTEMBER 15 TO DECEMBER 31, 1977**

D. E. Sawyer, H. K. Kessler,
and H. A. Schafft

Electron Devices Division
Center for Electronics and Electrical Engineering
National Bureau of Standards
Washington, D.C. 20234

July 1978

~~Final~~

Prepared for
Department of Energy
Washington, D.C. 20545



NBS Interagency Report NBSIR 78-1488

U.S. DEPARTMENT OF COMMERCE, Juanita M. Kreps, Secretary
Dr. Sidney Harman, Under Secretary
Jordan J. Baruch, Assistant Secretary for Science and Technology
NATIONAL BUREAU OF STANDARDS, Ernest Ambler, Director

CONTENTS

	Page
Preface	iv
Executive Summary	1
1. Introduction	2
2. Proposed Applications of the Laser Flying-Spot Scanner to Solar Cells	3
2.1 Overview of Some Cell Problems	3
2.2 Spatial Variation of Cell Response	4
2.3 Magnitude and Spatial Variations in Cell Emitter Sheet Resistance	5
2.4 Variations in Grid-Metallization Ohmic Contact	9
3. Work Performed During Reporting Period	10
3.1 Development of Solar Cell Device and Material Mea- surement Techniques	10
3.1.1 Laser Flying-Spot Scanner Modifications	10
3.1.2 Equipment for Light-Biasing Cells	12
3.1.3 Analysis	13
3.2 Workshops and Symposia	18
4. References	19
Appendix A	20
Appendix B	23

LIST OF FIGURES

1. Silicon $p-n$ junction diode photoresponse	6
2. Items a through c explain the variation in photoresponse with increasing frequency and distance from the top elec- trode depicted in figure 1	8
3. Solar cell clamping and rocking unit attached to the micro- scope cross-slide stage	11
4. Representation of the two-dimensional parasitic resistance- capacitance nature of a solar cell	14
5. The one-dimensional analog of the cell between a pair of grids shown in figure 4	16

PREFACE

This work was conducted as a part of the Semiconductor Technology Program of the National Bureau of Standards (NBS). This program serves to focus NBS research to enhance the performance, interchangeability, and reliability of integrated circuits and other semiconductor devices including solar cells through improvements in measurement technology for use in specifying materials and devices in national and international commerce and for use by industry in controlling device fabrication processes. This research leads to carefully evaluated and well-documented test procedures and associated technology. Special emphasis is placed on the dissemination of the results of the research to the appropriate technical community. Application of these results by industry will contribute to higher yields, lower cost, and higher reliability of semiconductor devices. Improved measurement technology also leads to greater economy in government procurement by providing a common basis for the purchase specifications of government agencies and, in addition, provides a basis for controlled improvements in fabrication processes and in essential device characteristics.

The segment of the Semiconductor Technology Program described in this quarterly report is supported by the Division of Solar Technology of the Department of Energy (DoE) under DoE Task Order A054-SE of Interagency Agreement EX-77-A-01-6010. The contract is monitored by Dr. Donald L. Feucht, Chief of DoE's Advanced Materials R&D Branch. The NBS point of contact for information on the various task elements of this project is Dr. David E. Sawyer of the Electron Devices Division at the National Bureau of Standards.

Certain commercial equipment, instruments, or materials are identified in this report in order to adequately specify the experimental procedure. In no case does such identification imply recommendation or endorsement by the National Bureau of Standards, nor does it imply that the material or equipment identified is necessarily the best available for the purpose.

Measurement Techniques for Solar Cells

QUARTERLY REPORT

September 15 to December 31, 1977

By

D. E. Sawyer, H. K. Kessler,
and H. A. Schafft

EXECUTIVE SUMMARY

This report covers research performed in the period September 15 to December 31, 1977 on the Program on Solar Cell Measurement Technique Development and Other Services by the Electron Devices Division of the National Bureau of Standards. The objectives of the program are to assist the DoE thin-film photovoltaic effort by developing solar cell device and material measurement techniques using the NBS-developed laser flying-spot scanner, and by assisting DoE in organizing and hosting appropriate workshops and symposia and providing general consultation and liaison services.

In this report several proposed applications of the laser scanner* for solar cells are described: measuring the spatial variation in cell response for various levels of bias light to map the behavior of the short-circuit photocurrent and the open-circuit photovoltage over the cell area, measuring magnitude and spatial variation in cell emitter sheet resistance, and determining emitter metallization regions making poor ohmic contact. Some additions and slight modifications were made to the scanner this first quarter to enhance its usefulness for examining solar cells. These include addition of lower magnification microscope objective lenses with longer working distances that allow the scanning of cells between the metallization stripes. These lenses also provide space for inserting fiber-optic light-guides for cell light-biasing. In addition, a cell mounting

* The scanner is described in Appendix B in enough detail so that the research described in this and subsequent reports can be understood without going outside this series.

stage was constructed. This stage uses vacuum to hold the cell and incorporates micrometers to adjust the plane of the cell with respect to the scanning beam and the reflected-light optical path.

Means for achieving high-intensity light-biasing were investigated. A high-pressure gas-discharge xenon lamp, similar to those used in solar simulators, was tried, but it generated an excessive amount of noise amplitude, modulating the lamp output and producing radio-frequency noise in the system to about 35 MHz. A quartz-halogen incandescent lamp, however, is expected to be adequately quiet when energized with a stable power supply.

The case of the scanner scanning between parallel "emitter" metallization stripes with a line of light modulated at high frequencies was analyzed. It is shown that the minimum-to-maximum signal ratio depends only on the modulating frequency, the (reverse-biased) junction capacitance (assumed spatially constant), and the emitter sheet resistance. The modulating frequency is known and the capacitance can be measured nondestructively. The analysis predicts that the emitter sheet resistance can be obtained by fitting the analytical value for the minimum-to-maximum ratio to the experimentally observed ratio.

The first workshop, Stability of (Thin-Film) Solar Cells and Materials, has been planned. This workshop is scheduled to be held May 1 to 3, 1978 at the National Bureau of Standards, Gaithersburg, Maryland.

1. INTRODUCTION

This report covers work performed in the period September 15 to December 31, 1977 on the Program on Solar Cell Measurement Technique Development and Other Services by the Electron Devices Division of the National Bureau of Standards under Task Order A054-SE of Interagency Agreement EX-77-A-01-6010.

The objectives of the program are to assist the DoE Advanced Materials R&D Branch photovoltaic effort in the following ways:

1. by developing solar cell device and material measurement techniques using the laser flying-spot scanner originally developed at NBS for use on integrated circuits and discrete transistors, and
2. by assisting DoE in organizing and hosting appropriate Workshops and Symposia, and by providing general consultation and liaison services.

Several proposed applications of the laser scanner for solar cells are described in section 2. Activities and accomplishments in both project areas during this reporting period are described in section 3. The outline of the first workshop is presented in Appendix A. Because this is the first quarterly report for the program, it is felt that its usefulness would be enhanced by a description of the laser scanning equipment. The scanner is described in enough detail in Appendix B so that the research described in this report and others to come can be understood without the reader needing to supplement these reports with other publications.

2. PROPOSED APPLICATIONS OF THE LASER FLYING-SPOT SCANNER TO SOLAR CELLS

2.1 Overview of Some Cell Problems

The requirements placed on terrestrial solar cells developed for DoE's Photovoltaic Program are unique in that a combination of adequate efficiency, low cost, and long life is demanded. Satisfying this set of requirements means that some serious problems have to be faced and overcome. Some of the cells which are leading contenders for wide-spread deployment may be made from poorly understood materials by fabrication techniques which history has shown can sometimes lead to inexplicable periods during which cells of adequate performance cannot be provided. An alternate approach is to use relatively expensive but well-understood materials such as single-crystal silicon or gallium arsenide, using only small amounts, and to rely on low-cost reflectors or Fresnel lenses to collect and focus the sunlight on the cell with concentration ratios of up to several thousand. The adequate design of a concentrator solar cell

can be a formidable problem. An appropriate analysis would begin with a device model suitable for computer simulation which would be both three-dimensional and allow the device parameters to vary in their values over this space. There are disadvantages to this approach, however. One is that the comprehensiveness of the model could obscure the cause and effect relationships between device parameter values chosen and overall cell efficiency. That is, the possible usefulness of the computer results in predicting what should be done to improve the cell may be obscured by the many quantities one could vary; it is not known on an *a priori* basis which quantities are important and must be specified accurately, and which quantities may be neglected for the sake of simplicity, to obtain a solution which may lead to better design insight. A third important class of cells, nonconcentrator types made from single-crystal materials, employs fabrication techniques which are quite similar to those developed by the integrated circuit industry. One significant difference between solar cells and integrated circuits is that the solar cell "emitter" (that portion above the *p-n* junction) is quite thin to enhance the cell response in the blue region of the spectrum, typically less than a half a micrometer in the more recent efficient designs. This means that a uniform and low-resistance contact to the emitter is more difficult to achieve for silicon solar cells without shorting through than it is for integrated circuits where the emitters may be several times as thick. The laser flying-spot scanner can help examine several of these problems, and appropriate scanner utilizations are sketched below.

2.2 Spatial Variation of Cell Response

It would be extremely useful, especially for concentrator cells, if one could measure the spatial uniformity of the cell over its surface. This could provide a check of the cell's design and fabrication steps. We will discuss in this first of the laser scanning activity reports how the scanner can be used in a rather simple manner to do this. It can reveal those portions of a cell which are not as effective as other parts in producing load power under illumination, and the scanner can present this information in a quantitative manner so as to allow an ac-

curate assessment of the cell deficiencies. This is a straightforward scanner application. The technique described can be used for any cell composition, and it will provide information badly needed for concentrator cell design and assessment. It can also be used to obtain a better understanding of the behavior of nonconcentrator cells, both conventional *p-n* junction single-crystal ones and cells made using structures and materials of a more exploratory nature. The technique itself is very simple. The cell is spot-scanned while it is uniformly illuminated by a bias light that can be increased step-wise in intensity. Under these conditions, the scanner display screen will present a map of the small-signal, or incremental, cell response. By scanning with various cell load values between zero ohms (the cell termination for measurement of short-circuit photocurrent) and infinity (the cell termination for measurement of open-circuit photovoltage), one could obtain maps which when compared with one another show the variation of these important parameters as the laser beam scans the photosensitive surface. The maps can further be interpreted to yield desired information about the cell's point-to-point operation. Establishing the validity of this measurement technique would be extremely valuable to the solar cell community. One obvious utilization is that it would allow one to compare solar cell design theory and experiment so that one may determine which of the many parameters that would be included in a two- or three-dimensional computer analysis are really important to specify and control.

2.3 Magnitude and Spatial Variations in Cell Emitter Sheet Resistance

The photomicrograph in figure 1a shows the silicon chip used for the first laser scanning observations of lateral (sheet) resistance. There are nine diodes, each about 250 μm on a side, formed by planar diffusion into *p*-type silicon of about 5 $\Omega\cdot\text{cm}$ resistivity. The diffusion was *n*-type and the junction depth was about 1 μm . These values of junction depth and bulk resistivity are close to those used for commercial silicon solar cells. The nine-diode chip was bonded to a header using con-

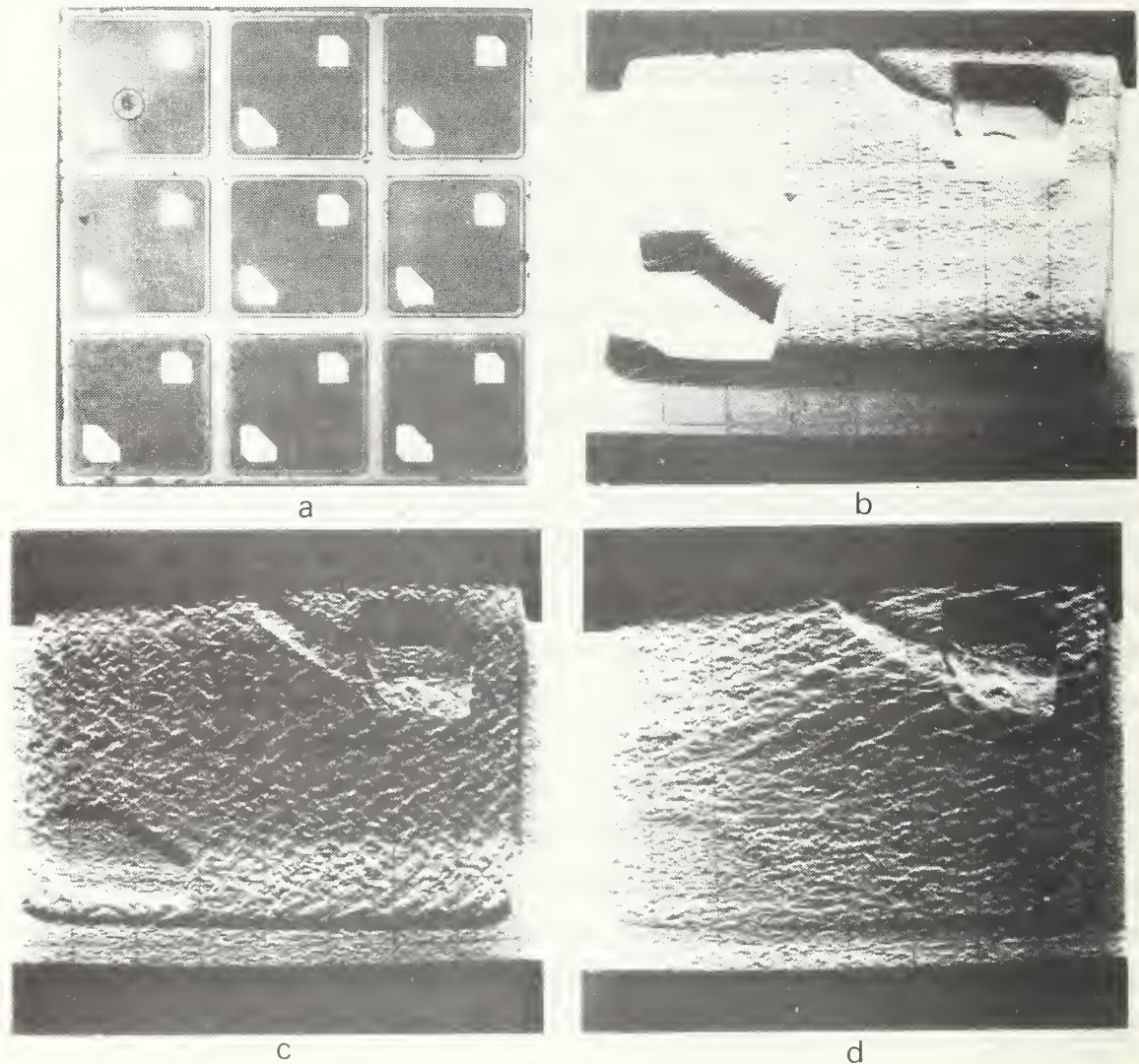


Figure 1. Silicon p - n junction diode photoresponse. The diode scanned is the central one in the upper left array of nine. The upper right photograph, figure 1b, is the photoresponse to unmodulated $0.633\text{-}\mu\text{m}$ light and with the diode reverse biased 5 V. The figure 1c photograph is for the same conditions except that the screen now displays the diode response to the light component modulated at 500 MHz, and the figure 1d photograph is the 1.0-GHz response.

ventional techniques, and a lead connecting one of the two ohmic contacts on the central diode was run to a header post.

The other photographs in figure 1 are photographs of the scanner display screen with the central diode scanned using laser light of wavelength $0.633 \mu\text{m}$ and with a diode reverse bias of 5 V. The presentation mode is a mixture of the conventional z-axis, i.e., intensity modulation along with vertical deflection of the horizontal scan lines by the same signal.

The photograph shown as figure 1b is the diode's response to unmodulated light; it is the small-signal dc or "video" diode response. The photograph shown as figure 1c is the response to the 500-MHz modulated component from the same laser and with the same bias conditions, while the photograph shown as figure 1d is the corresponding 1.0-GHz response. The gain of the display screen was adjusted to maintain the same maximum vertical deflection for all three photographs. This maximum occurs at the edge of the bonded contact. It is seen that the 500-MHz and 1.0-GHz photoresponses from portions of the diode away from the bonded contact drop off with increasing frequency and distance.

Figure 2 can be used to explain the results shown in figures 1b through 1d. Figure 2a is a cross section through the diode and figure 2b is the corresponding one-dimensional electrical representation of the diode. The diffused emitter region is represented by a distributed resistor and the junction transition region by a distributed capacitor. One would expect such a network to behave in the manner observed: the signal to the radio receiver would decrease with increasing signal frequency and distance of the laser excitation from the bonded contact, as sketched in figure 2c, because the attenuation due to the distributed resistance-capacitance line increases with these quantities. There are three independent variables for a given cell geometry: the signal frequency, the capacitance per unit area, and the sheet resistance. The sheet resistance is the only unknown; this is the quantity one would like to measure and it should be obtainable by fitting the measured response with the analytical solution appropriate for the cell geometry. It is noteworthy that this proposed method for sheet resistance measurements on

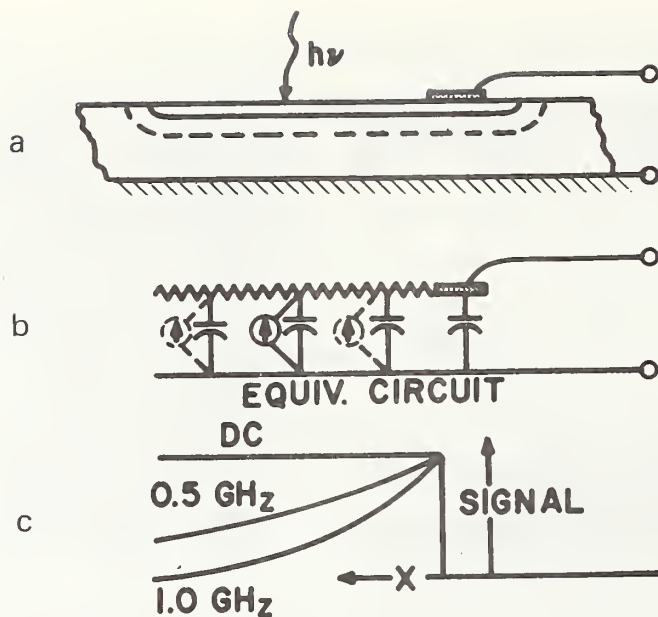


Figure 2. Items a through c explain the variation in photoresponse with increasing frequency and distance from the top electrode depicted in figure 1: the structure acts as a distributed resistance-capacitance transmission line and the response variation can be described in terms of the incremental resistance and capacitance line parameters.

completed cells is unique in that it requires the use of contacts which are normally a part of the cell, and that it is completely nondamaging to the cell.

For real cells, the analytic complexities are greater than that for the single one-dimensional line. The excitation is better represented by a volume with radial symmetry than by a mathematical line, but these realities should not introduce insurmountable analysis problems. For example, solar cell grids are at least a few millimeters apart. For light modulated at frequencies which are in the range of 500 MHz, the complex diffusion length in the semiconductor, e.g., silicon, shrinks to the order of a few micrometers, a distance somewhat larger than the one-half micrometer radius of the light spot in the NBS scanning system, but tiny in comparison with the grid spacing. Thus, for any realistic analysis, the spot can be considered a point source, and this simplifies the required analysis.

The experimental technique described above should also reveal variations in the sheet resistance of the (top) diffused layer. These variations can be a problem and may significantly affect solar cell output power, particularly for cells made from the more exploratory semiconductor materials in which inhomogeneities may be expected. Variations in sheet resistance due to any cause would be revealed by variations in the parameter chosen to fit the experimental data (the cell response) over the active area. After the analysis for the uniform sheet resistance case has been completed, an analysis may then be conducted to establish the range of sheet resistance variations which one may expect to reasonably detect.

The capacitance of solar cells made from the more exploratory materials may also vary over the cell area. Analyses of resistance-capacitance transmission lines such as those representing the distributed nature of solar cells usually produce answers in terms of resistance-capacitance products, and so one might conclude that the method then would not yield unambiguous values for sheet resistance variations. However, spatial variations in junction capacitance may be controlled independently by varying the cell bias voltage. The incremental sheet resistance is not a strong function of this voltage, but the capacitance per unit area is, and it probably may be made to vary in a predictable manner to allow the spatial variations in resistance and capacitance to be obtained independently.

2.4 Variations in Grid-Metallization Ohmic Contact

The preliminary results shown in figure 1 suggest that the laser scanner can be used to detect locations where the grid metallization forms a poor ohmic contact with the diffused layer. For uniform ohmic contacts the photoresponse along the grids will be uniform; but in regions of poor ohmic contact, the photoresponse will be less than that observed near good contacts.

3. WORK PERFORMED DURING REPORTING PERIOD

3.1 Development of Solar Cell Device and Material Measurement Techniques

3.1.1 Laser Flying-Spot Scanner Modifications

Some modifications were made to the laser flying-spot scanner to enhance its usefulness for scanning solar cells. The modifications were made in the vicinity of the specimen stage. The microscope objective lens was changed to one having both a lower magnification, 2.5X as contrasted with the 8X one most frequently used for scanning integrated circuits. The lower magnification provides a longer working distance (45 mm) and allows most solar cells to be scanned from one grid-line to another without moving the cell. The longer working distance provides the space between the lens and the scanned specimen needed when fiber optic bundles are used to bias the cell with steady-state light while scanning. (The light-biasing work is discussed in section 3.1.2.)

Most of the devices previously scanned were ICs and discrete transistors. In general, they were easy to mount for scanning since most of these devices came equipped with pins or wire leads which could be inserted in appropriate sockets clamped onto the microscope specimen stage. The plane of the scanned device could be easily adjusted by bending the device leads so that the light reflected from surface features such as a metallization is directed toward the germanium photodiode used in the reflected-light circuit. However, neither the same holding arrangement nor the same method for aligning the reflected-light path is workable with the usual solar cell. The usual cell is flat, and if leads are an integral part, then they are not as a rule adequate for holding the cell. To solve this problem, the clamping and rocking unit shown in figure 3 was designed and constructed to fit between the solar cell and the microscope x-y cross-slide stage; this latter retains its original function of placing the scanned specimen into the horizontal plane. The upper part of the unit is a vacuum chuck having replaceable top plates to accommodate cells of various sizes. The rocking feature is controlled by the two micrometer heads which can be seen in the photograph. These

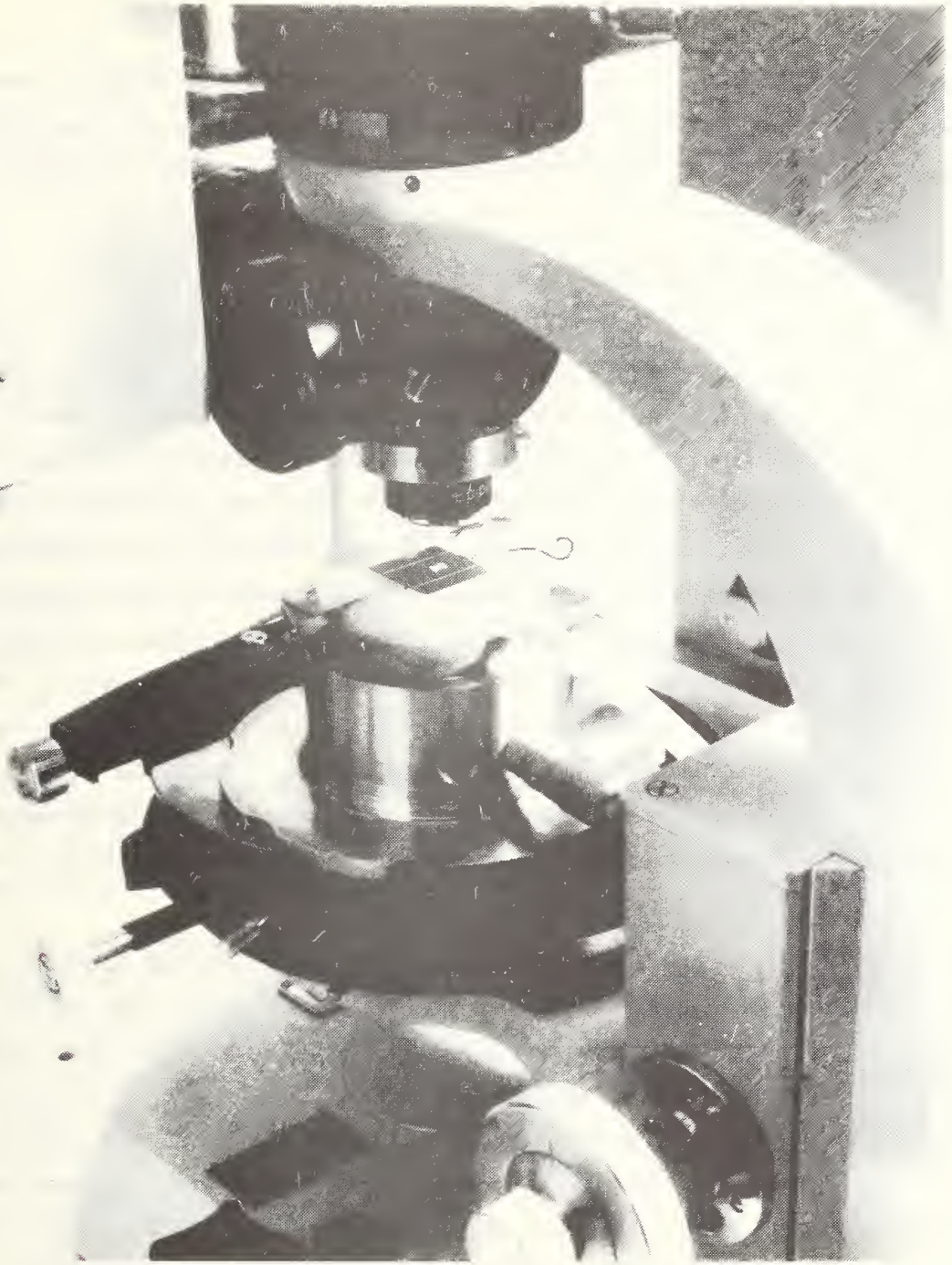


Figure 3. Solar cell clamping and rocking unit attached to the microscope cross-slide stage. Cell clamping is performed with a vacuum hold-down chuck magnetically held to the top plate of the rocking mechanism. Rocking (the orientation of the vertical axis) is controlled by micrometers. This photograph was made with the scanner in operation, and the pattern between grids approximately in the middle of the scanned cell is the raster of scanning light.

permit precise rotation of the vacuum chuck around the x- and y-axes to direct the reflected light to the germanium photodiode, and the chuck is spring loaded against the micrometer tips to maintain the settings of the micrometer heads.

3.1.2 Equipment for Light-Biasing Cells

One of the technical activities in the Program is to determine the small-signal photoresponse of various portions of cells while they are subjected to background light levels which are uniform in space and time. One should be able to interpret the small-signal scanned-cell photoresponse and determine the adequacy of the cell design and fabrication, tell a good deal about uniformity of the cell materials, and even localize cell defects. One interim specification for the illuminator is that it should produce, for nonconcentrator cells, a short-circuit current response equivalent to exposing the cell to an insolation of 20 suns at the cell-scanned area. Noise or modulation of the light, by e.g., an inadequately filtered lamp power supply, should be a minimum; otherwise the scanner signal-amplifiers will process this extraneous optical signal along with the cell response to the laser scanning spot and obscure the display information.

The light sources considered first were high-pressure gas discharge lamps such as are used in solar simulators. One such lamp was set up in a test bench and powered by a filtered dc source. Monitoring the light output with a photodiode revealed spikes and noise bursts which at times exceeded ten percent of the average light output and which had frequency components measurable to about 35 MHz. A dual-trace oscilloscope monitoring simultaneously the light output and the lamp voltage showed that the extraneous light signal originated within the lamp; undoubtedly this is associated with instabilities inherent in the gas discharge. Our conclusion is that, while such sources may be "quiet" enough for use in solar simulators where one is concerned with the average value of the light, they are not suitable for our needs.

Quartz-halogen sources were next investigated. A new model quartz-halogen high-intensity illuminator designed to be used with the same

model microscope as the one incorporated in the scanner was tried, but the results were disappointing; the short-circuit cell current for a small area (2 by 2 cm) cell was equal to only one-sun insolation. An examination of the optical path between the lamp and the specimen stage showed that although the illuminator was more than adequate for its intended usage, it was not designed for efficient utilization of the lamp's output, and the optics between the illuminator and the specimen constituted a high f-number system.

It is apparent that a light-bias system has to be tailored for the task. The approach which will be taken is to try a quartz-halogen incandescent lamp operating from a stable and low-ripple power supply, using flexible fiber-optic light pipes to direct the light to the cell area being scanned and a low f-number lens system to couple the lamp to the light pipes.

3.1.3 Analysis

This section continues the subject introduced in section 2.3: determination of the magnitude of and spatial variations in the cell emitter sheet resistance by scanning with laser light modulated at high frequencies.

Figure 4 is the representation of a solar cell showing the passive cell elements. Grids, shown by shading, are used to reduce the lateral resistance of the top, thin diffused region above the p - n junction, the so-called "emitter" region. These grid fingers are connected together and to a common top electrode which makes up one of the two electrical contacts to the solar cell, the other being an ohmic contact to the back surface of the cell wafer.

It is well known that the energy conversion efficiency of a cell may be severely reduced if the lateral resistance of the "emitter" is excessive, since all the photocurrent is constrained to flow laterally along the "emitter," and so almost all junction solar cells employ gridding to reduce this resistance [1]. Several gridding schemes may be employed. For example, the grids may be in the form of radial "spokes," or it may be in a crosshatch pattern, but the most common pattern is the "finger" configuration shown. This is the configuration which will be assumed in the

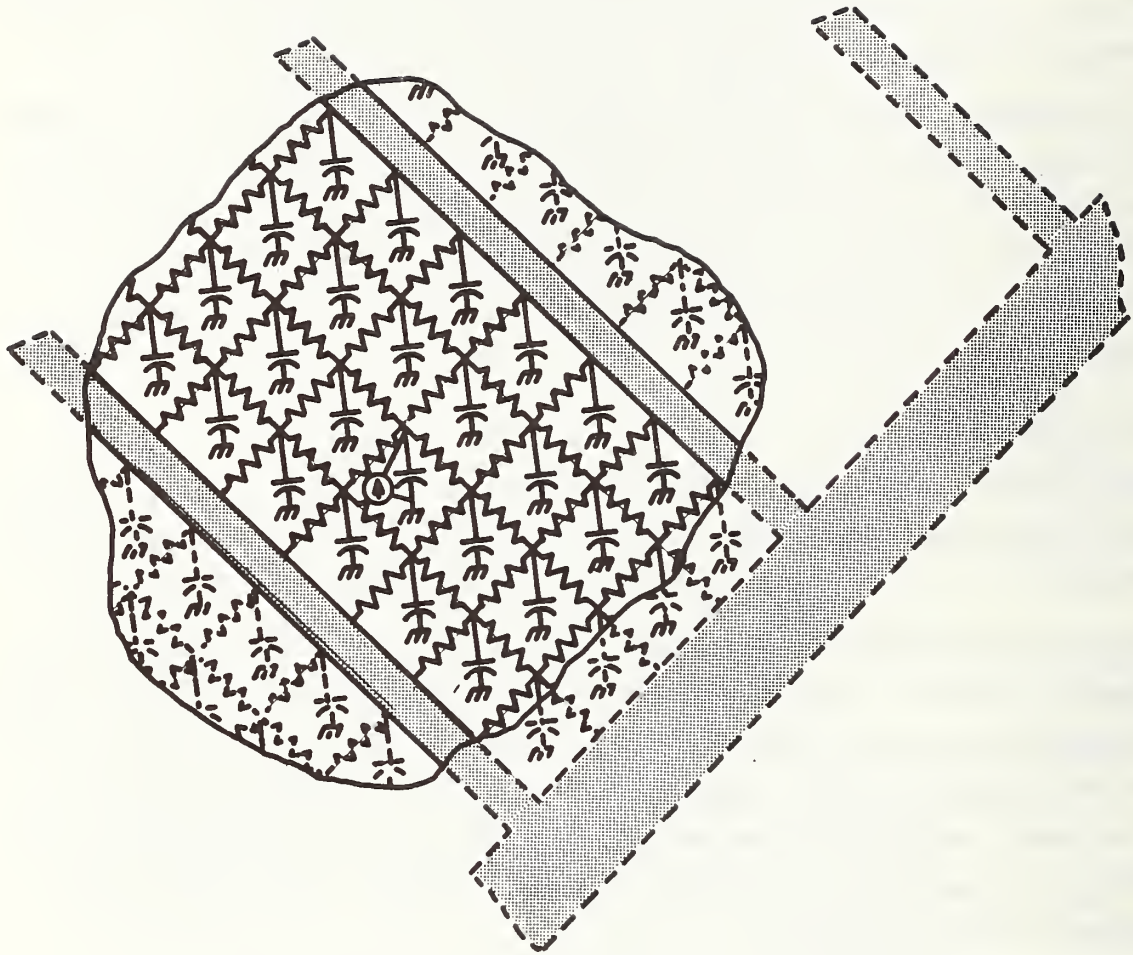


Figure 4. Representation of the two-dimensional parasitic resistance-capacitance nature of a solar cell.

analysis which follows. The purpose of this analysis is to determine the conditions under which the laser flying-spot scanner, using light modulated at high frequencies, can be used to determine in a nondamaging manner the sheet resistance of the "emitter." With this known through measurements made on the cells themselves, one can attempt to control its value on later cells and optimize cell performance. After techniques have been developed for *in situ* emitter sheet resistance measurements, one can then work toward developing techniques for measuring variations in this resistance. The emitter sheet-resistance measurement technique which will be described uses only the contacts to the cell (the electrode terminals) which are always an integral part of the completed cell.

The cell is assumed reverse biased in figure 4. (If it were not so biased, the equivalent circuit would include additional passive elements representing the junction diffusion admittance.) The state of affairs depicted corresponds to an instant in time when the laser spot is approximately midway between the two grid stripes. The device equivalent circuit is that of a distributed resistance-capacitance network due to the "emitter" sheet resistance and the transition-region capacitance of the reverse-biased *p-n* junction. The net result of carrier photogeneration due to the laser spot is to place a current generator across the transition-region capacitance just below the light spot [2,3,4], as shown in the figure. If the light is modulated, then the equivalent current generator will have both ac and dc components. (There will always be a dc component, because it is not possible for light to have an average value of zero!) Intuitively, one would expect that the ac voltage measured between the top and back electrodes to vary with the location of the light spot, reading a maximum just at the edge of a grid, and a common trough-shaped minimum midway between a pair of grids. One would expect this because of the symmetry of the grid pattern and because of greater attenuation of the signal current by the two-dimensional resistance-capacitance network as the distance between the light spot and its nearest grid line is increased.

For the geometry shown, the analysis is simplified if a line of laser light parallel to the grids is used, rather than a spot, and the scan-

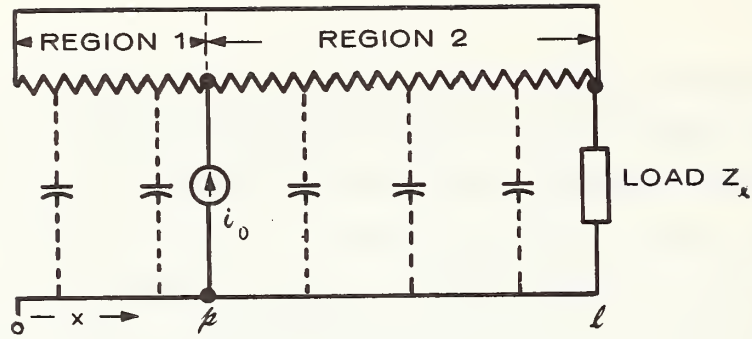


Figure 5. The one-dimensional analog of the cell between a pair of grids shown in figure 4. The current generator i_0 represents the equivalent current generator associated with the modulated laser light.

ning is performed by moving the light line parallel to itself. If the line is much longer than the separation of the grids, the problem can be treated as one dimensional, and figure 5 is the equivalent electrical circuit of the portion of the solar cell between two grids separated, edge to edge, a distance l . Scanning with a line of light will probably not be performed in the program. However, it is useful to analyze this one-dimensional case because the solution can be obtained in a closed-form expression which may be examined to anticipate the important results for the more realistic two-dimensional case. In figure 5 the scanning line is at a distance p from the edge of the left grid. It is clear that all such cell portions are equivalent. It is only necessary to analyze one, and the (as yet unspecified in value) impedance of the rest of the solar cell may be lumped with the cell terminating impedance (also unspecified) yielding a resulting load impedance Z_l .

The equations relating the line current $i(x)$ which flows in the plane of the "emitter," the voltage $v(x)$ across the line, the capacitance per unit length c of the line, the "emitter" lateral resistance r per unit length, the angular modulating frequency ω , and the coordinate distance x are easily derived and are

$$\frac{di(x)}{dx} = -j\omega cv(x) \quad (1)$$

$$\frac{dv(x)}{dx} = -i(x)r \quad (2)$$

where $j = (-1)^{1/2}$.

Differentiating eq (2) and substituting into eq (1),

$$\frac{d^2V(x)}{dx^2} - \beta^2V = 0 \quad (3)$$

where

$$\beta = (j\omega/\omega_0)^{1/2}, \quad (4)$$

and ω_0 is the angular frequency

$$\omega_0 \equiv (rc)^{-1}. \quad (5)$$

The general solution of eq (3) is

$$v(x) = Ae^{\beta x} + Be^{-\beta x}. \quad (6)$$

The constants A and B are chosen to satisfy the boundary conditions. From eq (2), the line current is

$$i(x) = \frac{\beta}{r} Be^{-\beta x} - \frac{\beta}{r} Ae^{\beta x}. \quad (7)$$

Two sets of equations similar to eqs (6) and (7) are required: one to represent the line to the left of p , and the other for the line to the right of p . Designating the quantities to the left by the subscript I, and to the right by the subscript II, and with i_0 representing the magnitude of the current generator due to the modulated laser light, the two sets of equations are solved subject to the boundary conditions

$$i_{II}(p) - i_I(p) = i_0 \quad (8)$$

$$v_I(p) = v_{II}(p) \quad (9)$$

$$v_I(0) = v_{II}(\ell) = Z_\ell [i_{II}(\ell) - i_I(0)]. \quad (10)$$

The voltage across the load Z_ℓ , i.e., the output voltage v_{out} for the scanning light line at the arbitrary position $0 \leq p \leq \ell$ is

$$v_{out} = i_0 Z_\ell \frac{\{\sinh[\beta(\ell - p)] + \sinh(\beta p)\}}{\{\sinh(\beta \ell) + \frac{2\beta Z_\ell}{r} [\cosh(\beta \ell) - 1]\}}. \quad (11)$$

As the laser light line is swept from one grid stripe to another, v_{out} undergoes a maximum-minimum-maximum excursion having the ratio

$$\frac{v_{out}^{(min)}}{v_{out}^{(max)}} = \frac{v_{out/p = \ell/2}}{v_{out/p = 0}} = 2 \frac{\sinh(\beta\ell/2)}{\sinh(\beta\ell)}. \quad (12)$$

It is noteworthy that this ratio does not depend on the effective load impedance Z_{ℓ} . All the quantities in eq (12), with the exception of r , are known, or can be found readily for the cell using nondamaging methods, and so selecting a value of r which brings eq (12) into agreement with the measured ratio $v_{out}^{(min)}/v_{out}^{(max)}$ yields the emitter sheet resistance.

3.2 Workshops and Symposia

An important part of this program is to set up workshops and symposia for DoE Headquarters on topics identified as important to the R&D New Materials Branch objectives.

The first workshop will be on the Stability of (Thin Film) Solar Cells and Materials and is scheduled for May 1 to 3, 1978 at the National Bureau of Standards in Gaithersburg, Maryland. One of its main purposes is to identify and discuss problems and obstacles to achieving 20-year life for terrestrial solar cells and to plan how these problems may be overcome by the use of test and measurement procedures designed to enhance the prediction and control of material and device stability.

This is a timely topic because DoE by 1985 will have committed itself to a restricted choice for thin-film materials and configurations [5]. An outline of the workshop, as it was structured during the reporting period, follows. The workshop was originally conceived by NBS to be a one-day affair, but as the needs of the thin-film solar cell community were examined more carefully it became obvious that one day would not be sufficient. After consultation with DoE Headquarters, it was decided that a more intensive workshop program was required to meet the needs of the solar community. As a consequence, it was decided to shift program priorities to emphasize the stability workshop activities. By the end of this reporting period, the workshop was planned to occupy two and one-half days.

The workshop outline detailed in Appendix A states its purpose and scope, as well as providing an overview of the specific discussion topics. It was mailed to members of the Workshop Steering Committee and discussed at a meeting of the Committee at DoE Headquarters on December 12, 1977.

4. REFERENCES

1. Hovel, H. J., Solar Cells, *Semiconductors and Semimetals*, Vol. 11, R. K. Willardson and A. C. Beers, Eds, (Academic Press, New York, 1975).
2. Gardner, W. W., Depletion-Layer Photoeffects in Semiconductors, *Phys. Rev.* 116, 84-87 (1959).
3. Anderson, L. K., Detection of Microwave Modulated Light, 1964 International Solid-State Circuits Conference Digest of Technical Papers, pp. 60-61.
4. Sawyer, D. E., A Study on $p-n$ Junction Photodetectors Utilizing Internal Parametric Amplification, Sperry Rand Research Report SRRC-PR-65-34, issued April 1965, Final Report of Work Performed 1 April 1964 - 31 March 1965. Prepared for the Department of the Navy, Bureau of Naval Weapons, Research Division (RRRE-3), Washington, DC. Contract No. N600 (19) 61770.
5. U.S. Department of Energy National Photovoltaic Program Plan, February 3, 1978.

APPENDIX A

Outline of the Workshop on Stability of (Thin-Film) Solar Cells and Materials

I. Purpose of the workshop

The purpose is to identify and discuss the problems and obstacles to achieving 20-year reliability for thin-film solar cells and to plan how these problems and obstacles may be overcome. The participants will also be asked if, in their opinion, cell stability testing should be an automatic part of the cell development work for cells which use exploratory materials or configurations (in some cases, this might be done by the same organization charged with developing the cell, but in most cases would be done by some other).

A. Specific and desired outcomes from the workshop

1. Definition of the problem areas,
2. Determining how to structure research leading to better cell and material stability,
3. Development of "standard," i.e., important, tests that should be performed, and
4. Guidelines for the design of stable cells.

B. A number of benefits to the Advanced Materials R&D photovoltaic community should accrue in the process of achieving the above goals, including

1. Identification of expertise in
 - a. stability considerations in general and
 - b. thin-film device stability,
2. Informing them on degradation phenomena,
3. Increasing their awareness of the need to "build in" cell reliability, and
4. Providing them with some of the resources needed to achieve built-in reliability and freedom from instabilities.

II. Scope of the workshop

The concern is with phenomena intimately related to the thin-film cell proper, i.e., occurring in the volume bounded by the semiconductor surfaces and the surfaces of the cell metallization. Analyses of general problems external to the active device, such as delamination of encapsulants and changes in optical transmission of window materials, will not be included. (The topics excluded should be covered adequately elsewhere - in DoE's single-crystal silicon and gallium arsenide array efforts, for example.) However, reliability and degradation problems

which are found for thin-film solar cells will not be excluded simply because they may also be found in devices which are other than those of concern to the Advanced Materials R&D Branch. This means, for example, that the widely observed degradation of solar cells due to metallization corrosion is a proper subject here, if the context is thin-film cells.

III. Workshop structure

A. Overview

The workshop will take the better part of two days and with a sequence which will begin with the experiences of other technical communities in engineering stability and freedom from the effects of degradation mechanisms and will move on to stability considerations appropriate to the thin-film solar cell community. This progression is chosen because it should provide the participants with the background and perspective needed to appreciate the ubiquitous and complex nature of the problem. It should also, by exposing the workshop participants to similar problems in these other fields, suggest means whereby solutions may be found. Most of the workshop talks will be invited, but participation of the audience will be encouraged.

B. Papers

The papers are expected to fall into the following three areas:

1. Papers which provide a perspective on the problem areas from the vantage point of work performed on more mature devices by larger technical communities (by the integrated circuit industry, and in the $p-n$ junction single-crystal silicon solar cell effort, for example);
2. Papers which address degradation and instability mechanisms appropriate to thin-film photovoltaic devices; and
3. Papers which recommend appropriate tests and screens.

C. Some suggested topics for the morning of the first day (the theme is "What we can learn from others")

1. Device stability, reliability and degradation-mode data accumulated for the DoD community: what this should teach the photovoltaic community, and how to make use of this accumulated experience. The talk would be given by a representative of the Rome Air Development Command or the Reliability Analysis Center.
2. The experiences of JPL, NASA/LeRC, Sandia in areas of general concern such as mechanical integrity, delamination of cell constituents, changes in optical properties of window materials, corrosion of cell metallization, etc.
3. Special concerns in concentrator cells.

4. Newer results suggesting that significant bulk/surface changes may occur in some silicon $p-n$ junction single-crystal cells.
- D. Some suggested topics for the afternoon of the first day (the theme is "What are (or should be) the particular concerns of the thin-film community")
1. Growth with time of oxides beyond initial, optimum thickness, in MOS "Schottky" cells,
 2. Nature of hydrogen bonding may determine stability of amorphous silicon cells,
 3. Field-aided copper migration, and cadmium diffusion, may degrade CdS/Cu₂S, or CdS/copper-ternary cells,
 4. General thin-film phenomena; for example, the consequences of grain boundaries such as enhanced diffusion, and
 5. Accelerated testing of thin-film materials and structures.
- E. The morning of the second day, working groups will develop position documents on, for example:
1. what are the degradation phenomena which one needs to test for,
 2. recommended test conditions, i.e., what are the tests which are appropriate to carry out,
 3. appropriateness of accelerated life testing, and
 4. the use of special test vehicles (test patterns) to magnify changes which would be occurring in the "real" cell, and so allow short-duration tests to predict the long-term cell changes.
- F. The summary session would be held in the early afternoon of the second day. This would:
1. summarize what has been learned, and
 2. present recommended test and measurement procedures designed to enhance the ability of one to predict material and device stability.

Laser Scanning of Active Integrated Circuits and Discrete Semiconductor Devices*

D. E. Sawyer, D. W. Berning, and D. C. Lewis**

Institute for Applied Technology
National Bureau of Standards
Washington, D.C.

The device laser scanning work conducted in the Electronic Technology Division of the National Bureau of Standards (NBS) is described. The scanner constructed at NBS is sketched briefly; this is followed by illustrations demonstrating its usefulness for determining on a point-by-point basis the inner workings of active semiconductor devices. The scanner is non-damaging to all devices tried and it has been used to map d.c. and high-frequency gain variations in transistors, reveal areas of the device operating in a non-linear manner, electronically map temperatures within devices, determine internal logic states in IC's and selectively change these states at will. It has also been used to perform hitherto impossible measurements on flip-chip bonded devices, that is, seeing the circuit electrical operation and the metallization pattern through the back side of the chip. Applications to other structures and devices including solar cells are suggested.

THE EFFECT OF DIRECTING LIGHT of energy somewhat greater than that of the band gap on a semiconductor is to create electron-hole pairs within the material which can be collected as a photocurrent. If the light is focused to a spot and moved over exposed semiconductor portions of a device, it is possible to learn a great deal about the internal operation of the device by interpreting the photoresponse. The interpretation is facilitated if the photoresponse is presented on the screen of a cathode ray tube whose electron beam is deflected in synchronism with the moving light spot since a "picture" of the photoresponse of the device is presented. Interpretation of the display can yield, on a point-by-point basis, information about the device which can be used to determine internal characteristics. This probing technique has applications in device testing, device design, and reliability. Provided that the photon energy of the light is less than a few times the band gap energy of the semiconductor one would not expect either short or long term device degradation to occur due to the light (provided of course that the optical power density at the specimen is not excessive). No device damage due to the flying-spot scanner has been observed.

Scanner Description

The scanner to be described here is based on previous work^{1,2,3} and several innovations. A schematic outline of the scanner is shown in Fig. 1; a photograph of the apparatus is shown in Fig. 2.

Light for the laser scanner is provided by either of two low power He-Ne cw lasers. The wavelength of one laser is 1.15 μm ; the wavelength of the second laser is 0.633 μm .

Mirrors M_1 and M_2 are used to fold the output from the 1.15- μm beam so that the scanner can be made more compact and rugged; mirror M_1 is used for the same purpose with the 0.633- μm beam. Mirror M_3 is used to select which laser output is to be used with the scanner; it can be used to block the 1.15- μm beam and simultaneously insert the 0.633- μm beam into the scanner, or it can be used to deflect the 0.633- μm beam out of the optical circuit of the scanner.

The analyzer shown at the output of the 0.633- μm laser in Fig. 1 is used to control the intensity of the radiation delivered to the device under test. Since the output of the laser is plane polarized, rotation of the analyzer can vary the transmissivity from 0 to 1. There is no intensity control on the 1.15- μm laser.

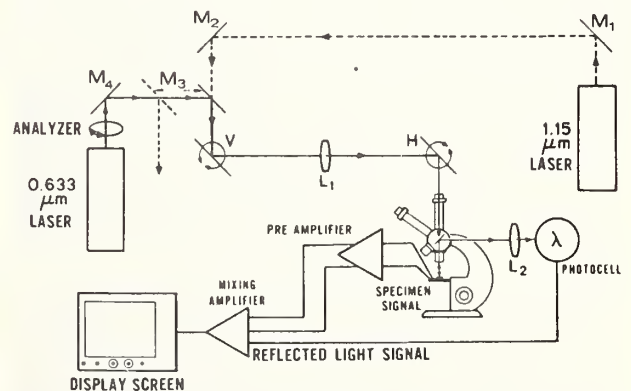


Fig. 1—The light and signal paths of the dual laser scanner.

*This work was conducted as part of the National Bureau of Standards program on Semiconductor Measurement Technology with principal funding from the Defense Advanced Research Projects Agency through ARPA Order 2397.

**Present address: Office of Naval Research, Washington, DC 22217.

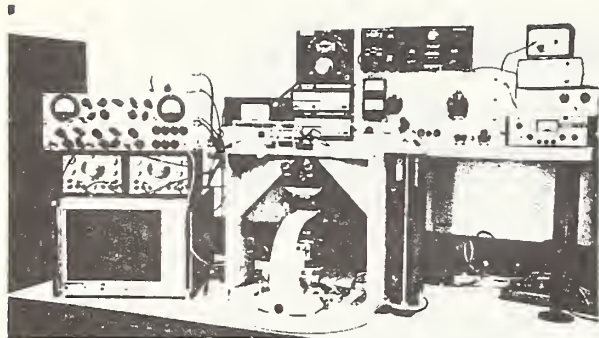


Fig. 2—Photograph of the laser scanner.

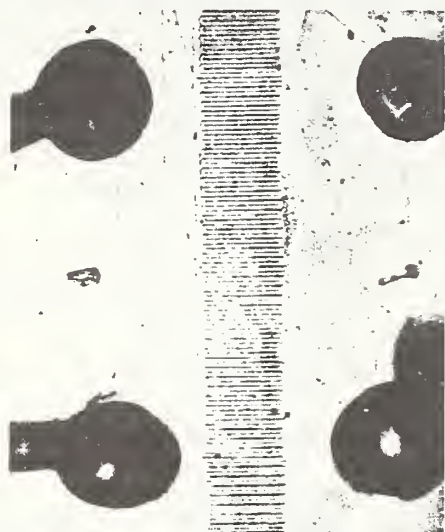


Fig. 3—Optical photograph of the surface topology for a microwave transistor consisting of four cells.

Mirrors V and H are electrically driven to provide orthogonal deflections of the light beam. Light from mirror H passes through a microscope and is focused to a spot on the device to be examined. The same electrical signals that drive mirrors V and H also deflect a spot on a cathode ray display screen in synchronism with the laser scan. The display screen is on the lower left of Fig. 1. The lens L_1 between the vertical and horizontal deflection mirrors refocuses the vertical deflection from V onto the horizontal mirror, H. The beam diverges from the horizontal deflection mirror, H, to form the scanning raster. The scan raster typically covers the same field of view that can be seen with the eye when the microscope is used in its customary manner. Light reflected from the specimen is used to identify the portion of the specimen being scanned. The reflected-light circuit uses a half-silvered mirror in the microscope which is an integral part of the microscope's vertical illuminator, a lens L_2 , and a photocell. Laser radiation reflected from any point on the specimen is directed by the half-silvered mirror onto the lens and is focused to a fixed point on the photocell. The photocell signal modulates the display screen to present a picture of the device surface topog-

raphy. Used this way, one could call the apparatus a "flying-spot microscope." The primary purpose of the reflected-light circuit is to permit correlation of the device response with surface features such as metallization areas. This is accomplished simply by mixing together the signals from the scanned specimen and the photocell. Alternatively, a color display screen has been used with the photocell signal fed into one color channel and the electrical signal(s) from the scanned specimen into the other(s). A recent publication⁴ describes in detail the construction and operation of the entire scanner.

Two lasers are used for a greater measurement flexibility. Visible or near-infrared radiation incident on silicon creates electron-hole pairs with a generation rate which exponentially trails off with distance into the material. The penetration depends on the wavelength of the incident radiation. The visible light from the $0.633\text{-}\mu\text{m}$ laser has a characteristic penetration depth of about $3\ \mu\text{m}$ in silicon.⁵ Because most modern silicon devices have their active regions within a few micrometers of the surface, the $0.633\text{-}\mu\text{m}$ laser is quite effective in exciting active regions of silicon operating devices. The intensity at the specimen can be varied to produce junction photocurrents over the range from about $10\ \text{pA}$ to about $0.1\ \text{mA}$.

Silicon at room temperature is almost transparent to the $1.15\text{-}\mu\text{m}$ infrared radiation from the second laser; the characteristic penetration depth of this radiation is about $1\ \text{cm}$.⁵ The infrared laser is used for three classes of measurements: 1) examination of the silicon-header interface; 2) device temperature profiling; and 3) examination of the device through the backside of the silicon chip. Each of these applications makes use of the penetrating nature of the radiation. In the first application, the reflected-light circuit is used to look through the silicon wafer and observe irregularities at the silicon-header interface in the "flying-spot microscope" mode. The second application makes use of the temperature sensitivity of the silicon absorption; a larger signal is produced on the display screen for those device portions which are warmer than others. Utilizing this sensitivity, one has an electronic technique for thermal mapping of devices which appears to have a number of advantages over the more traditional methods.⁶ The third application uses the penetrating infrared radiation to photogenerate carriers deep within silicon devices; this capability allows the operation of devices that are bonded face down (e.g., beam lead devices) to be examined.

Mapping of Device Electrical and Thermal Characteristics

Figure 3 shows photographs of the metallization pattern of a type 2N4431 UHF transistor. This widely available type is designed to furnish $5\ \text{W}$ at frequencies up to $1\ \text{GHz}$. There are four in-line cells electrically connected in parallel; these are shown in the left photograph. The total active area of the transistor is a rectangle $1.2\ \text{mm}$ long and $0.15\ \text{mm}$ wide. The emitter

and base fingers are interdigitated with the emitter fingers coming in from the right, and the base fingers coming in from the left. The finger metallization is $2\ \mu\text{m}$ in width, and the stripe separation is $8\ \mu\text{m}$. The metal stripe separation allows the active device regions to be accessible to laser irradiation. For the results that will be shown, the devices were scanned while they were connected and biased in the common-emitter configuration. The signal for the display screen was taken from a 60 ohm resistor which served as the collector load. For several of the transistors, it was found that regions of high temperature, so-called "hot-spots," would form within the acceptable operating range listed in the manufacturer's data sheet. This observation was used to aid in understanding the many things the scanner can tell us about the way a device really works. Figure 4 shows photographs of the display screen. The upper left image is the infrared response for a collector-emitter voltage of 26 V and a collector current of 250 mA. The transistor is operating just outside of the hot-spot region. Little of the incident optical energy is absorbed in the device active regions so the display screen signal is weak. The infrared response was actually quite uniform over the device, and the apparent nonuniformity captured in this photograph was due to system noise which had the effect of modulating the presentation of the photoresponse. The lower left photograph was made for the same scanning conditions but with the bias adjusted slightly to put the transistor into hot-spot operation.⁸ The region of enhanced photoresponse, the white area, is the hot-spot region as confirmed with the use of a passive infrared microscope. The photoresponse is proportional to the number of electron-hole pairs photogenerated in the device active region. For radiation from the infrared laser, which is lightly absorbed at room temperature, the number of pairs photogenerated increases with temperature because the optical absorption coefficient increases with temperature. This is due primarily to the well-known change in the silicon bandgap with temperature and an increase in the phonon population. It is possible to assign temperature values to this thermal-enhancement of the $1.15\text{-}\mu\text{m}$ response, and a paper describing the details is in preparation.⁷

The upper right photograph is for the same hot-spot conditions, but it was made using the response to the visible laser. Essentially all of the incident light is absorbed in the active regions at room temperature and so no enhancement in the hot-spot is observed.

During normal operation, each laser produces optical radiation at a series of discrete wavelengths centered about the nominal wavelength corresponding to the individual allowed axial modes of the laser. Self-mixing of these wavelengths modulates the light simultaneously at several frequencies. The modulation frequencies are multiples of a fundamental one, and for the particular visible laser used, the light is self-modulated at 500 MHz and 1.0 GHz to a degree adequate for determining the response of devices to light modulated at these frequencies. One inserts a radio receiver between the specimen

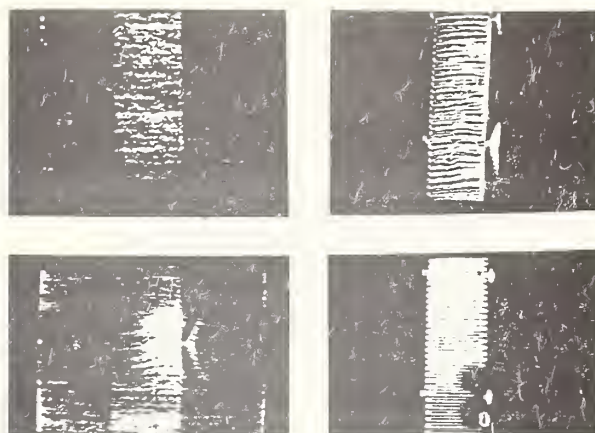


Fig. 4—Electrical responses of microwave transistor. Top left: infrared photoresponse outside the hot-spot regime; bottom left: infrared photoresponse in the hot-spot regime; top right: visible photoresponse in the hot-spot regime; bottom right: visible photoresponse with the modulated light at 500 MHz.

and the display electronics and tunes the receiver to the selected frequency.

The lower right photograph in Fig. 4 is for the same bias and optical wavelength as for the upper right photograph. In this case the radio receiver is used and the image produced is the response of the transistor to the component of the laser light modulated at 500 MHz. This image is interpreted as the spatial map of the 500-MHz gain of the transistor. It is well known that the hot-spot formation can influence high-frequency device gain.⁸ The hot-spot area is revealed quite dramatically, and it can be seen that there are actually two hot spots symmetric about a cell boundary.

By scanning a device with an electrical signal applied to its usual input port, one can map on the display screen the regions of the device which are operating nonlinearly at the signal frequency. All that is required is that an i.f. amplifier and detector, tuned to the difference frequency of the electrical signal and a laser mode beat, be inserted between the device output and the display screen.⁹ Nonlinearities can indicate stress points and so this mapping may be useful in predicting certain types of device failures. It may also be useful in selecting linear devices for applications in which many devices are used cascaded throughout a communications system; component nonlinearity in such applications is to be avoided since it may produce cross-talk between channels. For these reasons, this unique ability to map device nonlinearities should make the laser scanner invaluable for device design, testing, and reliability.

Internal Operation of Integrated Circuits

The results of scanning a type 7438 dual-input NAND gate IC with $0.633\text{-}\mu\text{m}$ light are shown in Fig. 5. The schematic of the bipolar IC appears in the upper right quadrant along with the truth table. The output transistor (the output is labeled Y) is normally in its high, or

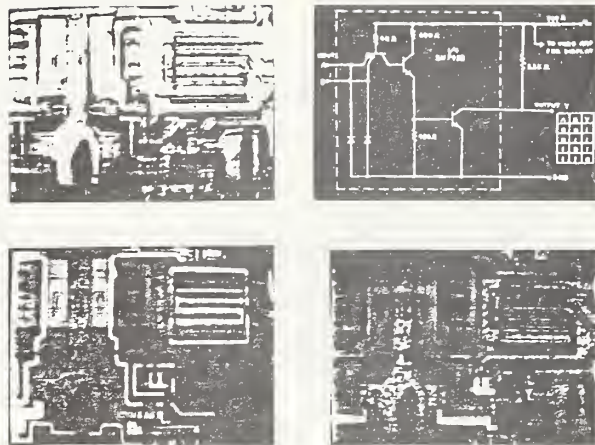


Fig. 5—Type 7438 dual-input NAND gate. Top right: schematic and truth table; top left: reflected-light image; bottom left: photoresponse superimposed on reflected-light image with output in high state; bottom right: photoresponse superimposed on reflected-light image with output in low state.

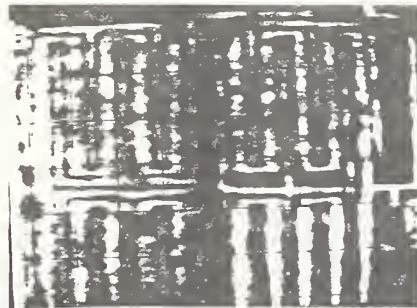


Fig. 6—Photograph of the display when scanning through the back side of a silicon-on-sapphire C-MOS device.

nonconducting state, and to switch it into its low state, i.e., into saturation, requires that both inputs A and B be in their high states. The overall NAND gate operation is specified by the trio of numbers representing A, B, and Y, in that order. As an example, the case in which A and B are high to cause the output to go low is listed in the table as 110. The top left photograph was generated solely by the scanner's reflected light circuit and it shows the metallization. The output transistor occupies the upper right quadrant. To reveal the NAND gate's internal operation, it was biased for normal service with a 330 ohm resistor inserted in the supply bus, and the voltage variation across this resistor during laser scanning modulated the display screen. A transistor operating with significant small-signal current gain will show a large photoresponse and consequently produce a bright image on the display screen. On the other hand, a transistor operating with little small-signal current gain, such as when it is in saturation, will produce almost no image. Thus, from the photoresponse of the elements in the circuit, the different logic states can be deduced. Naturally, changing the state of the NAND circuit yields a new photoresponse display of the active elements.

The photograph in the lower left quadrant of Fig. 5 is the superposition of the scanned IC's electrical response and the reflected-light metallization signal for the 001, 101, and 011 states; all give the same results. The output transistor is in its high state, and an appreciable photoresponse is obtained from portions of the base-collector junction not covered by metallization. The input transistor is located directly below the output transistor, and very little photoresponse is observed from it because no appreciable amplification of the photocurrent generated in the input transistor can occur unless the transistor is out of saturation, i.e., unless both inputs are in their high states.

For the photograph in the lower right quadrant of Fig. 5, the circuit state is 110, and the output transistor is in saturation with little photoresponse obtained from it. The input transistor is out of saturation, and the two L-shaped areas, one under another, below the output transistor are the unobstructed base-collector junction regions around the emitters. The illuminated region to the left is the inter-stage transistor, and the horizontal bar below this is the 4K ohm load for the input transistor.

MOS IC's also have been inspected with the laser scanner. In addition to observing the states of all the logic elements, and the states of the input-output circuits in a shift register, it has been possible to change the state of a desired logic element from 0 to a 1 or vice versa nondestructively with the laser spot.¹⁰ This ability could have far-reaching implications for the testing of LSI circuits, particularly for testing those portions that are embedded, i.e., with no direct connections to external leads.

Examining IC's Through the Wafer

In the work described so far, the scanning light beam was incident on the side of the chip containing the active circuit. But, it is possible to scan a device using penetrating light such that the light enters the back surface and passes almost entirely through the chip before being partially absorbed in the device active region or reflected by the metallization. The 1.15- μm He-Ne laser wavelength is nearly optimum for accomplishing this in silicon devices. Because of the penetration, photocurrents from deep within the chip may contribute to the overall response.

Light scattering due to back surface irregularities must be minimized in order to maintain resolution, and this requires either that the back side be smooth, or that a drop of liquid be placed on the surface having an index of refraction approximately equal to that of the semiconductor.

Back surface scanning was successfully tried on three different types of devices: C-MOS on sapphire, bulk C-MOS, and a bulk bipolar circuit.

The C-MOS on sapphire circuit, a type 4007, was scanned from the back side using visible light ($\lambda = 0.633 \mu\text{m}$) because sapphire is optically transparent. A drop of light oil was deposited on the back of the de-

vice substrate to provide an optically smooth surface. The photograph of the scanner display shown in Fig. 6 was obtained using the reflected light signal mixed with the photoresponse of the inverter. Of the six transistors shown in this figure, only the lower right hand one was electrically connected. The five brightly lit stripes are the gate area of the electrically "on" device.

The bulk silicon C-MOS integrated circuit was also a 4007; however, since the substrate was silicon, it was necessary to use the 1.15- μm wavelength. Figure 7 shows the reflected light image. No oil was needed as the back side was a polished surface.

The third device was a beam-leaded bulk silicon bipolar 709 operational amplifier. In this case oil was deposited on the back of the device die to provide an optically smooth surface. Figure 8a shows the 1.15- μm scanning image obtained when the amplifier was connected to provide a gain of 10 and with 0 V input. The reflected-light signal is superimposed on the photoresponse. Figure 8b shows the device for the same conditions except that the input voltage is now -1.5V , a value sufficiently large to saturate the 709.

These three examples demonstrate a capability of the scanner which can be very useful when metallization on the top of the chip obscures the underlying device active regions but these regions are accessible from the back, or when it is desired to inspect devices bonded into frames or packages "face down" with direct access to the active surfaces blocked by mounting materials.

Application to Photodetectors and Solar Cells

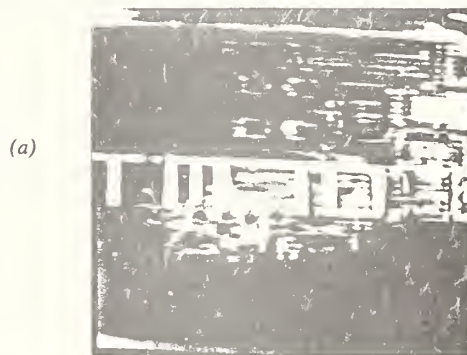
The laser scanner is an obvious candidate for analyzing photodetector operation. Devices made from a number of materials, including silicon and indium arsenide, and designed for optical communication, have been scanned with unmodulated light, and light modulated at frequencies up to 1.2 GHz, to study gain and spatial response variations. These devices have been both those that utilized internal (avalanche) gain, as well as those which utilized simple photodetection. Even vacuum devices have been scanned; measurements have been made of the uniformity of cathode response for a 931-A photomultiplier to 0.633- μm light modulated at 120 MHz. Experimental solar cells designed for space applications have been laser scanned and the results compared with those obtained with a scanning electron microscope in the electron-beam-induced-current (EBIC) mode. The defects located with the SEM were also found with the laser scanner, in these preliminary experiments. The scanner described in this paper should also be useful in observing variations in solar cell response with light level, and this could be invaluable for cell design. This could be done by scanning the cell with a "small signal" laser while at the same time exposing the cell uniformly to an auxiliary source which would be varied step-wise in intensity.¹¹

Summary

The scanner work described makes use of the fact



Fig. 7—Photograph of the display when scanning through the back side of a bulk silicon C-MOS device with the infrared laser.



(a)



(b)

Fig. 8—Images obtained when scanning a commercial flip-chip operational amplifier with the infrared laser. (a) Input at 0 V. (b) Input at -1.5V .

that semiconducting materials are photosensitive as part of their basic nature. Thus, semiconductor devices such as diodes, transistors, and entire integrated circuits made from these materials can be studied using optical radiation. The effect of the optical radiation is to generate electron-hole pairs in a non-damaging way within the specimen. These current-carriers can stimulate device behavior by taking the place of signal current-carriers which are normally supplied by leads fixed to the device. In contrast to signals applied via the leads, which are fixed in position, the optical excitation can be moved

Laser Scanning

over the surface and within the bulk, and the response of the structures can be studied on a point-by-point basis to learn the inner workings of the device.

In several cases, the scanner has been used to observe device phenomena which one has not been able to study before. The scanner can map the flow of logical information in MOS and bipolar IC's. It can map the operation of transistors at ultrahigh frequencies; it can electronically map the temperature distribution; it can pinpoint the portions of operating devices which are operating in a non-linear manner; and it has the unique ability to look through the back side of silicon chips to observe circuit operation.

References

1. Potter, C. N., and Sawyer, D. E., "A Flying-Spot Scanner," *Rev. Sci. Instrum.* vol. 39, 180-183 (1968).
2. McMahon, R. E., "Laser Tests IC's with Light Touch," *Electronics*, vol. 44, 92-95, (April 12, 1971).
3. Beiser, L., "Laser Beam Scan Enhancement through Periodic Aperture Transfer," *Applied Optics*, vol. 7, 647-650 (1968).
4. Sawyer, D. E., and Berning, D. W., "A Laser Scanner for Semiconductor Devices," NBS Special Publication 400-24, February 1977. Available from the Superintendent of Documents, U.S. Govt. Printing Office, SD Cat. No. C13.10: 400-24.
5. Dash, W. C., and Newman, R., "Intrinsic Optical Absorption in Single-Crystal Germanium and Silicon at 77° and 300°K," *Phys. Rev.*, vol. 99, 1151-1155 (1955).
6. Sawyer, D. E., and Berning, D. W., "Thermal Mapping of Transistors with a Laser Scanner," *Proc. IEEE*, vol. 64, 1634-1635 (1976).
7. Sawyer, D. E., and Lanyon, H. P. D., "Determining Silicon Device Temperatures By Measuring the Thermally-Enhanced 1.15 μm Photoresponse," to be published.
8. Oettinger, F. F., and Rubin, S., "The Use of Current Gain as an Indicator for the Formation of Hot Spots Due to Current Crowding in Power Transistors," *IEEE 10th Annual Proceedings, Reliability Physics*, 12-18 (1972).
9. Sawyer, D. E., and Berning, D. W., "Mapping Nonlinearities Over the Active Regions of Semiconductor Devices," *Proc. IEEE*, vol. 64, 1635-1637 (1976).
10. Sawyer, D. E., and Berning, D. W., "Laser Scanning of MOS IC's Reveals Internal Logic States Non-destructively," *Proc. IEEE*, vol. 64, 393-394 (1976).
11. Lanyon, H. P. D., Worcester Polytechnic Institute, Worcester, MA, private communication.

June 1977/SOLID STATE TECHNOLOGY

U.S. DEPT. OF COMM. BIBLIOGRAPHIC DATA SHEET		1. PUBLICATION OR REPORT NO. NBSIR 78-1488	2. Gov't Accession No.	3. Recipient's Accession No.
4. TITLE AND SUBTITLE Measurement Technique for Solar Cells: Quarterly Report September 15 to December 31, 1977			5. Publication Date	6. Performing Organization Code
7. AUTHOR(S) D. E. Sawyer, H. K. Kessler, and H. A. Schafft			8. Performing Organ. Report No.	
9. PERFORMING ORGANIZATION NAME AND ADDRESS NATIONAL BUREAU OF STANDARDS DEPARTMENT OF COMMERCE WASHINGTON, D.C. 20234			10. Project/Task/Work Unit No.	11. Contract/Grant No. Task Order A054-SE
12. Sponsoring Organization Name and Complete Address (Street, City, State, ZIP) Advanced Materials R&D Branch Division of Solar Technology Department of Energy 20 Massachusetts Avenue, N.W. Washington, D. C. 20545			13. Type of Report & Period Covered Interim Sept. 15-Dec. 31, 1977	
15. SUPPLEMENTARY NOTES			14. Sponsoring Agency Code	
16. ABSTRACT (A 200-word or less factual summary of most significant information. If document includes a significant bibliography or literature survey, mention it here.) This is the quarterly report of the work performed in the three month period September 15 - December 31, 1977. The objectives of the program are to assist the DOE thin-film photovoltaic effort by developing solar cell device and material measurement techniques using the NBS-developed laser flying-spot scanner, and by assisting DOE in organizing and hosting appropriate workshops and symposia and providing general consultation and liaison services. Several possible applications of the laser flying-spot scanner to solar cells are discussed including measurement of the spatial variation in cell response versus bias light to map cell behavior under various insolation conditions, measuring magnitude and spatial variation in cell emitter sheet resistance, and determining emitter metallization regions making poor ohmic contact. Additions and modifications to the optical and mechanical portions of the scanner made to enhance its usefulness for solar cells are described. An analysis is presented for scanning, with light modulated at high frequencies, the most common solar cell geometry. The results predict that the cell emitter sheet resistance can be obtained by analyzing the laser display screen presentation. Scanner background information is included in an appendix. The outline of the Workshop on the Stability of (Thin Film) Solar Cells and Materials is presented. This workshop is scheduled to be held May 1-3, 1978 at NBS, Gaithersburg.				
17. KEY WORDS (six to twelve entries; alphabetical order; capitalize only the first letter of the first key word unless a proper name; separated by semicolons) Device measurements; laser scanning; light-biasing; metallization; ohmic contacts; reliability; semiconductor measurements; sheet resistance; solar cells; solar cell stability.				
18. AVAILABILITY <input checked="" type="checkbox"/> Unlimited <input type="checkbox"/> For Official Distribution. Do Not Release to NTIS <input type="checkbox"/> Order From Sup. of Doc., U.S. Government Printing Office Washington, D.C. 20402, SD Cat. No. C13 <input type="checkbox"/> Order From National Technical Information Service (NTIS) Springfield, Virginia 22151		19. SECURITY CLASS (THIS REPORT) UNCLASSIFIED		21. NO. OF PAGES 30
		20. SECURITY CLASS (THIS PAGE) UNCLASSIFIED		22. Price

